# Detection of photons in the HERA-B RICH

P. Križan
*J. Stefan Institute and University of Ljubljana, Slovenia*
for the HERA-B RICH group[1]

*Abstract*

The tests carried out with the photon detector of the ring imaging Cherenkov detector for the HERA-B experiment are reviewed. Results of the on-the-bench tests of the employed photomultiplier tubes are reported together with the early commissioning measurements with the HERA proton beam.

## I. Introduction

The HERA-B experiment [1] aims at measuring: CP violation in $B^0 \to J/\psi K^0_S$ and $B^0 \to \pi^+\pi^-$ decays, $B^0_s\bar{B}^0_s$ mixing and $B\bar{B}$ decays with two leptons in the final state. The $B$ mesons will be produced in collisions of 920 GeV/c protons with a fixed target. The target consists of 8 wires in the halo of the proton beam in order not to disturb experiments measuring $ep$ collisions.

One of the essential components of the spectrometer is the ring imaging counter (RICH), with the prime function of separating kaons from pions [1, 2, 3, 4]. In what follows we shall briefly describe the essential components of the RICH counter, and will then discuss in detail the detection of photons.

## II. The HERA-B RICH

The main purpose of the Ring Imaging Čerenkov counter (RICH) in the HERA-B experiment is the tagging of the $B$ meson flavour. Tagging of the of $B^0$ or $\overline{B^0}$ meson is accomplished by identifying the charged kaon into which the associated B meson decayed. The momentum distribution of charged kaons, resulting from decays of the B mesons, is shown in Fig. 1. Identifying the charged kaon essentially means separating it from the pion of the same momentum. Since the momentum is accurately measured in other components of the HERA-B detector, the separation in mass is equivalent to separation in velocity.

Perfluorobutane gas ($C_4F_{10}$) has been chosen for HERA-B RICH radiator, since it combines relatively high refractive index, $n(3.3eV) - 1 = 1.330 \cdot 10^{-3}$ and low dispersion, $\Delta n/\Delta E(3.3eV) = 3 \cdot 10^{-5}\frac{1}{eV}$. In this gas the Čerenkov radiation threshold momenta for pions and kaons are at 2.7 GeV/c and 9.6 GeV/c, respectively. For $\beta = 1$ particles, the Čerenkov angle is 51.5 mrad, while the $\pi - $K difference in Čerenkov angle is 6 mrad

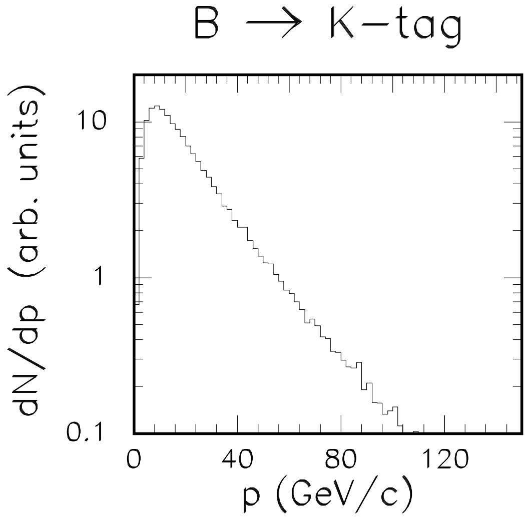


Fig. 1 The momentum distribution of charged kaons produced in decays of $B$ mesons associated to the production of a $B^0$ or $\overline{B^0}$ meson by proton nucleus interactions at HERA-B.

[1]The HERA-B RICH group is a collaboration of the University of Texas at Austin, University of Barcelona, LIP Coimbra, DESY Hamburg, University of Houston, J. Stefan Institute, Ljubljana, University of Ljubljana and Northwestern University.

at 20 GeV/c and falls to 0.9 mrad at 50 GeV/c.

In a fixed target experiment such as HERA-B where one has to deal with intense fluxes of charged particles, special care has to be taken when designing a ring imaging Čerenkov counter. The design choices are governed by the following criteria. To achieve the necessary performance, a sufficient number of photons (at least 20) has to be detected for each ring image [1]. This requirement fixes the length of a gas radiator to a few meters. The high rate capability of the photon detector requires some kind of chamber with pads, and therefore limits the resolution to a few milimeters. This, in turn, together with the required high resolution in the measurement of the Čerenkov angle (better than 1 mrad) sets the focal length value to several meters. Last but not least, the delicacy of the photon detector with a very low detection threshold, necessary to count single photoelectrons, requires the photon detector to be kept out of the solid angle for charged particles and conversion products.

The resulting set-up of the counter is schematically shown in Fig. 2. The two spherical mirror halves are tilted, i.e. the center of curvature of each mirror half is displaced relative to the target position, by which photons are reflected to photon detectors well outside the charged particle flux.

The 108 m$^3$ vessel for the $C_4$F$_{10}$ gas radiator has been constructed out of stainless steel, except for the particle entry and exit windows (1 mm Al) and the photon exit windows (UVT perspex). Also, two beam shrouds close the gas volume around the two beam pipes for protons and electrons. The purification and circulation system for the $C_4$F$_{10}$ gas has been constructed at CERN and was commissioned at DESY.

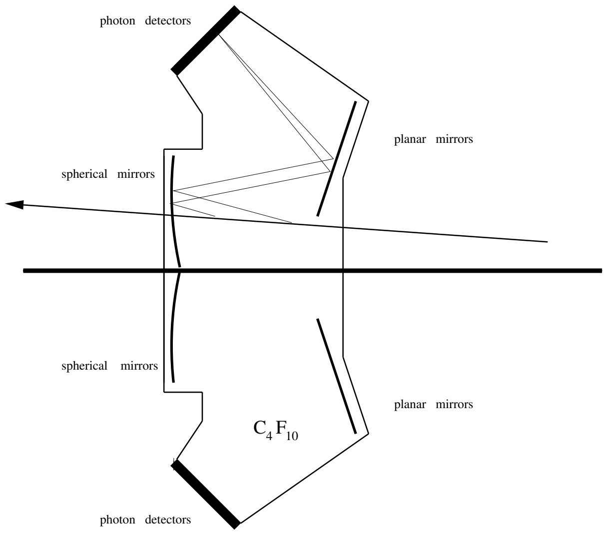

Fig. 2 *The HERA-B RICH.*

It is worth noting that the initial filling of the volume amounts to about 1100 kg of $C_4$F$_{10}$.

Two mirror systems, a spherical and a planar one, are made of hexagonal and rectangular units, respectively. The hexagonal mirror segments with 11.4 m radius of curvature have been produced from 7 mm thick grinded glass. The mirror quality has been determined upon delivery [5] by measuring for each segment the radius of curvature, and the fraction of reflected light, as well as by recording a Ronchi image to check the homogeneity of the mirror surface. The reflectivity was required to exceed 85% in the wavelength interval 250 nm - 600 nm. Each spherical mirror segment is supported at three points, two of which can be moved, and are motor driven via a transmission mechanism with a feed through to the exterior of the vessel. The planar mirrors are made of float glass, thus being significantly cheaper at the required optical quality. By making use of the data gathered on all the mirror segments, it was possible to group them in the tiling scheme according to their optical quality and resolution requirements [6].

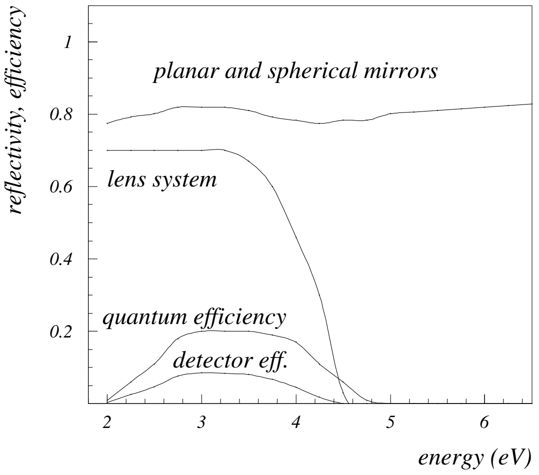


Fig. 3 *Reflectivity of planar and spherical mirrors and the detection efficiency of the photon detector as a function of photon energy. The photon detector efficiency is a product of the photomultiplier tube quantum efficiency, the photoelectron detection efficiency and the transparency of the optical system.*

## III. PHOTON DETECTOR

Initially, two wire chamber based photon detectors were considered, a CsI photocathode in a MWPC and a TMAE based detector with 10 cm deep, 8 x 8 mm$^2$ unit cells. After considerable success of on-the-bench and beam tests [7, 8, 9], the detectors were tested in a high rate environment as expected in the HERA-B experiment. Both wire chamber based detectors had to be abandoned; the TMAE detector showed a prohibitive decrease of avalanche gain due to aging effects [10, 11], while the CsI photocathode could not be routinely produced and maintained with sufficiently high quantum efficiency in addition to problems with rates in excess of a few kHz per pixel [12, 13].

The final photon detector consists of Hamamatsu multianode R5900 M16 and M4 photomultiplier tubes, which became available just at the time when it was realised that an alternative solution is needed. The M16 version has 16 pads of 4.5 x 4.5 mm$^2$ each, with a 12-stage, metal-foil dynode system [14]. The M4 version has 4 pads of 9 x 9 mm$^2$ each, and 10 dynodes. The quantum efficiency of the photocathode with borosilicate window has a broad plateau in the wavelength region between 300 nm and 500 nm with a maximum value of 20% (Fig. 3). The UV-extended version has a UV transparent window, which shifts the low wavelength cut-off to about 250 nm. The other PM characteristics such as the required cathode high voltage ($\leq$ 1000 V), the current amplification ($10^7$), dark current ($\sim$ 1 nA), pulse rise time (0.8 ns), transit time spread (0.3 ns) [14], are also satisfactory.

The outer dimensions of the PMT are 28 x 28 mm$^2$, so the photocathode occupies only about 30% of the surface. Due to the smaller photocathode surface compared to the photomultiplier cross section, a two lens demagnification system (2:1) was designed (Fig. 4) [15]. The lenses are made of UVT perspex with high transparency over most of the wavelength region where the photocathode is sensitive (Fig. 3). The angular acceptance of the optical system is also satisfactory and is uniform for incident angles below about 110 mrad [16]. In addition to increasing the active area the lens system also adjusts the required pixel size in the central detector region (9 x 9 mm$^2$) to the PMT pad size 4.5 x 4.5 mm$^2$. The outer detector region with lower occupancy and looser resolution requirements uses the M4 version of the tube with two times larger pads (9 x 9 mm$^2$) with the same lens system, such that the pixel size amounts to 18 x 18 mm$^2$.

The base board accepts four PMT's and provides positioning. In addition it houses the voltage divider, signal lines and the front-end electronics consisting of 16-channel boards based on the ASD8 chip [17]. In Fig. 5 a photograph of a fully equipped basic module for the M16 photomultiplier tubes is presented.

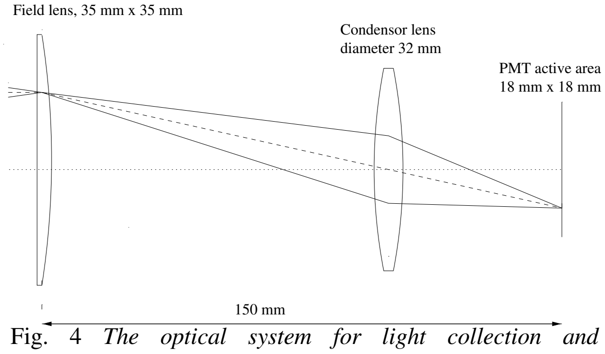


Fig. 4 *The optical system for light collection and demagnification. The two rays shown in full line correspond to photons with incident angles of* $\pm 100$ *mrad.*

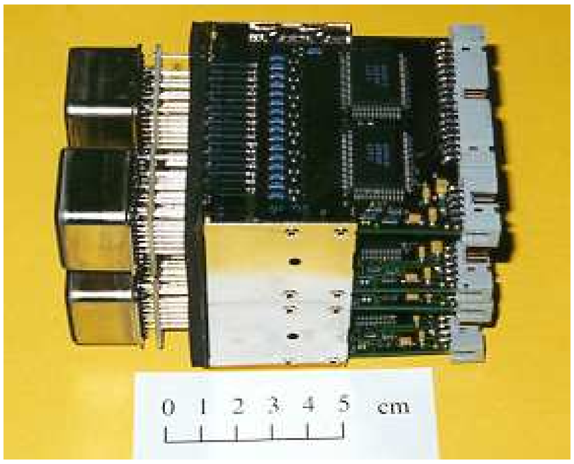


Fig. 5 *Fully equipped photomultiplier basic module housing Hamamatsu R5900 photomultiplier tubes type M16.*

In order to reduce the contribution of spherical aberration to the overall resolution of the Čerenkov angle, an optimal surface of the Čerenkov photon detector has been calculated [18, 19]. Each half-detector (upper and lower) consists of 5 flat supermodules placed in order to approximate the optimal surface, which is close to the shape of a flattened (ellipsoidal) cylinder. Such an arrangement also ensures better acceptance for the Čerenkov photons, which should be incident onto the flat supermodules at angles below 110 mrad.

From the data available on the quantum efficiency, mirror reflectivities, window and optical system transmissions (see Fig. 3), one calculates the merit factor $N_0 = 43\,\mathrm{cm}^{-1}$, such that the expected number of photons for particles approaching the velocity of light amounts to $N_{det} = N_0 L \sin^2\vartheta = 31$ with $L = 2.7$ m and $\vartheta = 51.5\,\mathrm{mrad}$.

## IV. Measurements and Results

### *A. Multianode PMT as a single photon counter*

In the initial set of measurements [21] the single photon counting properties of the tube were investigated, in particular the efficiency for single photon detection as well as the background count rate. In this phase three multianode PMT's were tested; one with borosilicate glass window (ser.no. 6A19C4) and two with UV transparent windows (ser.no. 5M26C6 and ser.no. 6C22C5). The tubes were of the 16-channel photomultiplier tube assembly type which includes a voltage divider circuit (Hamamatsu type H6568).

In the experimental set-up shown in Fig. 6 it was established that the tube allows for a good single photoelectron detection as may be seen in Fig. 7. The

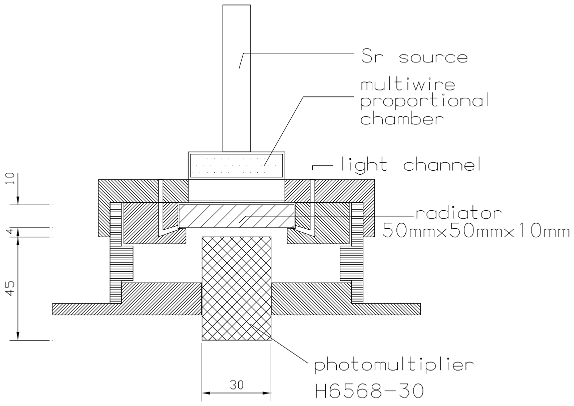


Fig. 6 *The set-up for testing the PMT properties on the bench. Čerenkov photons, emitted by* $^{90}Sr$ $\beta$ *particles in a solid radiator, are used as a stable light source [22].*

average pulse height on each of the pads is shown in Fig. 8. These data were obtained by allowing a small leak of daylight into the crystal radiator from which the photon reached the photocathode more or less uniformly illuminating its surface.

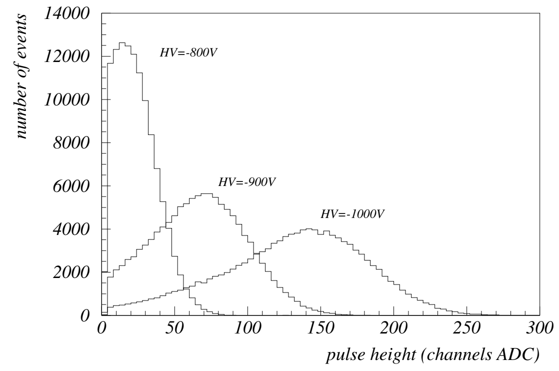


Fig. 7 *The measured pulse height distributions of the M16 PMT due to single photoelectrons for different high voltage values.*

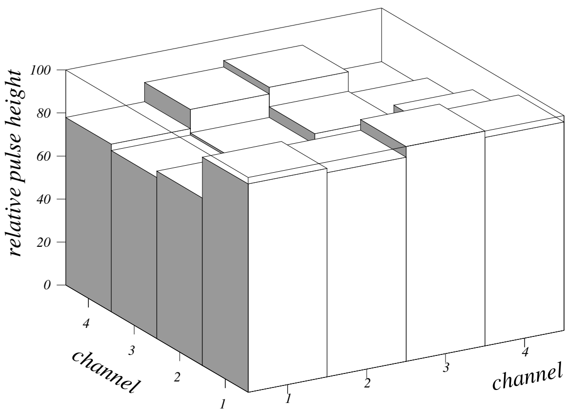


Fig. 8 *Lego plot of the average single photoelectron pulse heights normalised to the pad with the largest average pulse height.*

The bleeder chain was optimized by varying the composition of the 13 resistors [23]. Very little dependence of rate at the high voltage plateau was seen when varying the fraction of 1 MΩ to 560 kΩ resistors. Somewhat better results were obtained with the first three steps of 1 MΩ resistors, followed by ten 560 kΩ resistors. This bleeder chain was then adopted for the M16 photomultiplier tube. For the M4 photomultiplier a similar voltage divider was chosen, where again the first three resistors had twice the value of the other eight.

Cross talk has been estimated by observing simultaneous pulses on adjacent pads, when the pulse on one pad has been recorded to be above a certain threshold. The pulse height spectra, triggered by pad number 7 are shown in Fig. 9. The cross talk is estimated from this figure to be 0.2% between direct neighbours and only 0.1% between diagonal neighbours.

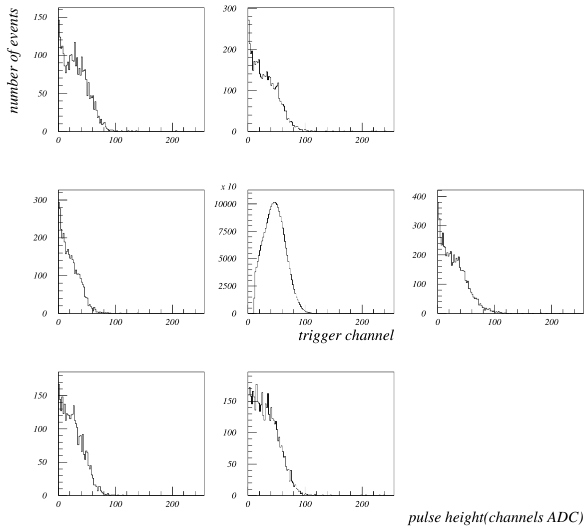


Fig. 9 *Cross talk has been measured by triggering with one of the channels and observing simultaneous pulses on six neighbouring channels.*

Ageing was studied [21] by illuminating the photocathode pads with a 5 W neon bulb through a small hole at one side of a 1 m long, 10 cm diameter black plastic tube with the PM on the other side. No reduction of the 3 MHz counting rate has been observed over a 30 day period of continuous illumination and operation.

## *B. Results of quality assessment tests*

Tests of all the 2300 PMT's (1543 M16's and 762 M4's) have been made in the laboratory prior to the installation in the photon detector [24]. The apparatus employed is similar to the one shown in Fig. 6. Again Čerenkov photons from $\beta$ electrons of the $^{90}$Sr source were used as a stable light source. In this case four

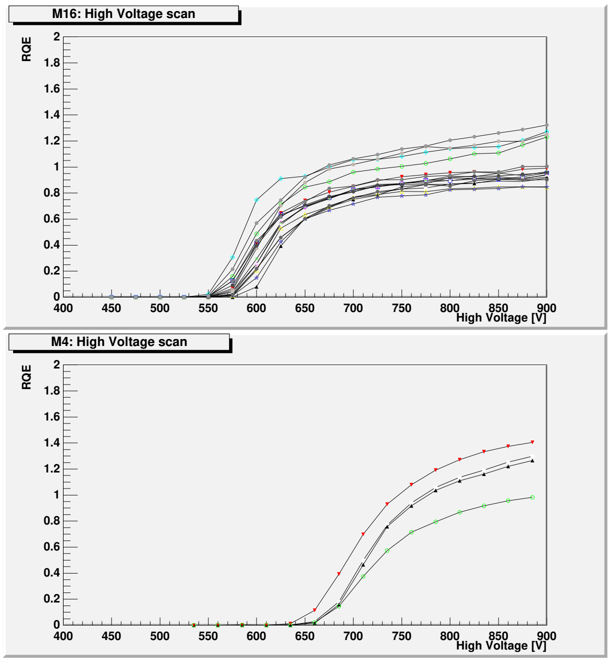


Fig. 10 *Dependence of the suitably normalized rate (channel count rate divided by 1000 and 4000 for M16 and M4 PMT's respectively) as a function of the high voltage for all channels of a representative M16 (above) and M4 (below) photomultiplier tube.*

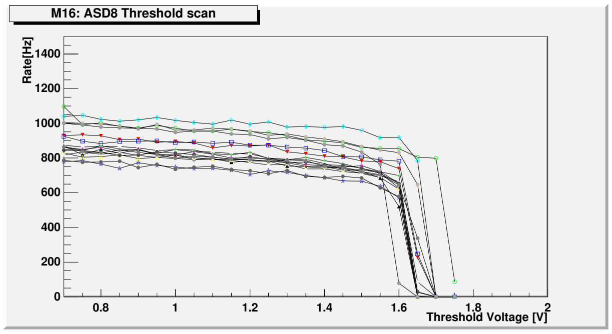


Fig. 11 *Dependence of the count rate on the threshold voltage for a typical M16 photomultiplier tube.*

tubes were tested at the same time, of which one was used as a reference. For each photomultiplier tube, a high voltage scan, the rate variation with threshold, and the background rate were recorded (Figs. 10-12). On the basis of these tests, the photomultipliers have been grouped according to similar high voltage characteristics, allowing all PMT's within a group to be connected to the same high voltage, thus maximising the efficiency for the given, much smaller number of independent HV channels [20]. The results obtained

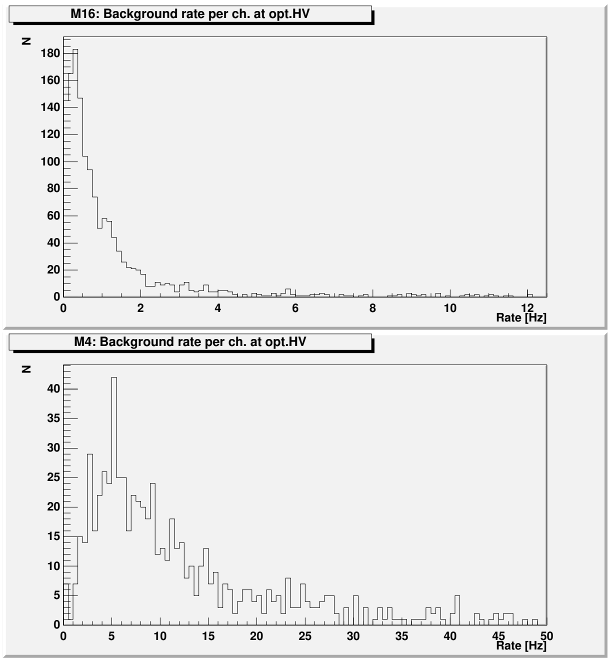


Fig. 12 *Distribution of M16 (top) and M4 (bottom) channels depending on their background count rate.*

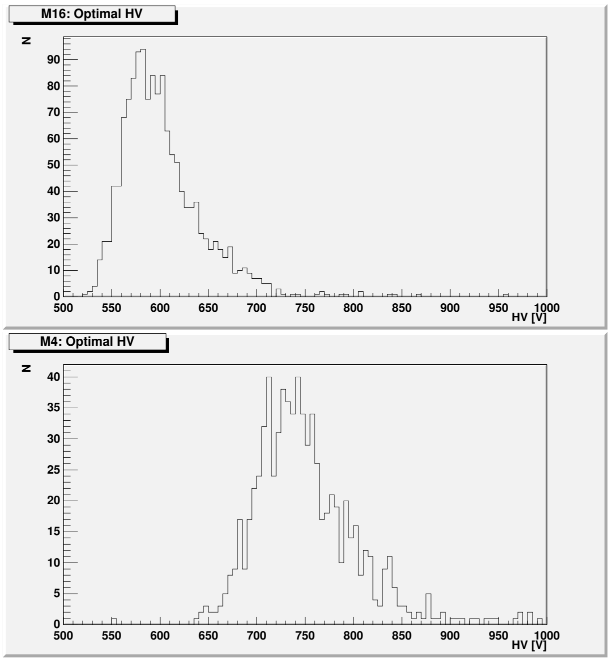


Fig. 13 *Distribution of M16 (top) and M4 (bottom) photomultipliers depending on the value of their recommended high voltage.*

for the optimal high voltage as well as for the relative PMT sensitivity were compared to values provided by the manufacturer, and a good agreement was found [24].

Fig. 13 gives the distribution of M4 and M16

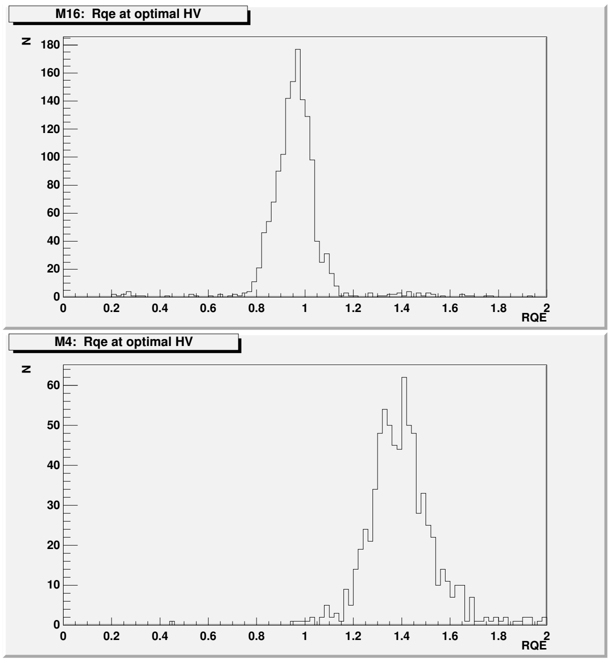


Fig. 14 *Distribution of M16 (top) and M4 (bottom) photomultipliers according to their normalized count rate (RQE) at the recommended voltage.*

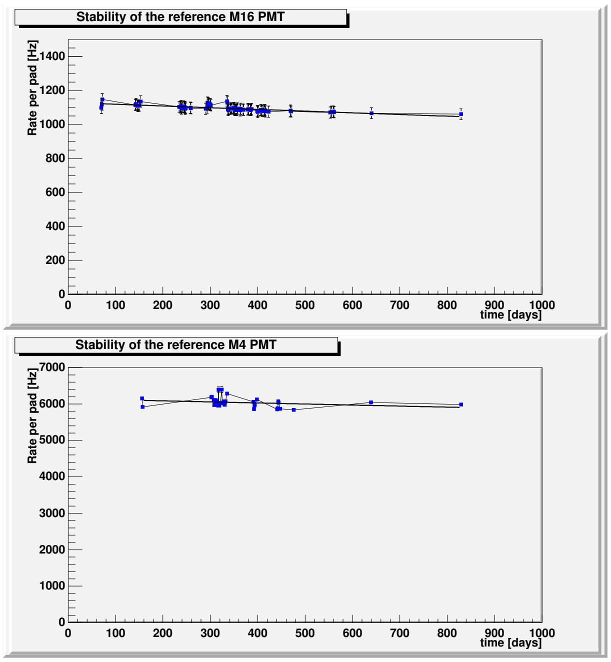


Fig. 15 *The time dependence of the count rates of the reference photomultipliers; M16 (top diagram), M4 (below). The curves represent the radioactive decay of $^{90}$Sr.*

photomultipliers versus their recommended high voltage value as obtained in the quality assessment tests. This value is seen to be larger for M4's than for M16's, which is a consequence of the smaller number of dynodes (10 for M4's compared to 12 for M16's). The distributions of photomultipliers depending on their normalized count rate (channel count rate divided by 1000 and 4000 for M16 and M4 PMT's respectively) at the recommended value of high voltage are shown in Fig.14 separately for M16's and for M4's.

Finally Fig.15 shows the time dependence of the rate per channel of the reference M4 and M16 photomultipliers in the quality assessment tests. The count rate decrease is consistent with the known decay rate of the $^{90}$Sr source.

From the quality assessment tests relative surface sensitivity of each tube could be determined, after correcting for a slightly non-uniform illumination of the surface. An example for each of the PMT types is shown in Fig. 16.

To further investigate the variation of sensitivity over the photomultiplier surface, a scan was carried out for selected PMT's by using a light beam spot of about 20 $\mu$m diameter [25]. From Fig. 17 the pad and dynode channel structure can clearly be seen.

## C. Test measurements in situ

With the photon detectors in their proper position in the HERA-B spectrometer, the photomultipliers cabled to the readout system and with freon as Čerenkov radiator, the commissioning of the system became possible. Fig. 18 gives the count rate versus high voltage for some M16 and M4 photomultipliers. It is seen that the curves measured in-situ with the HERA proton beam agree nicely with the $^{90}$Sr source measurements. The occupancy is shown in Fig. 19, where the region occupied by M16 PMT's is clearly distinguished from the region occupied by M4 PMT's. We also note that only about 0.3% of the nearly 30.000 channels were found to be noisy, and were excluded

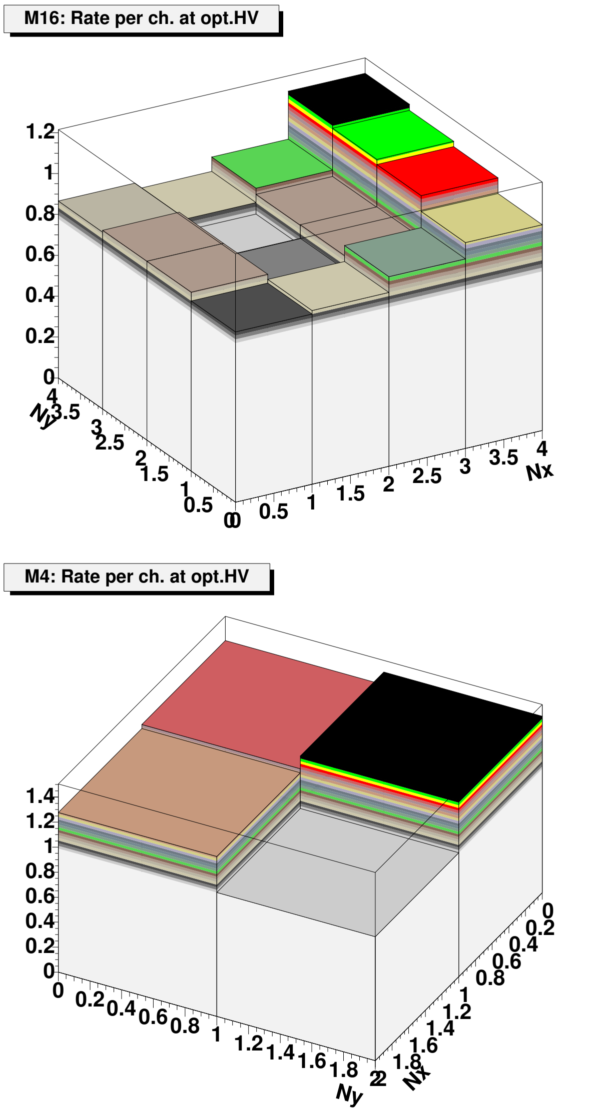


Fig. 16 *Relative sensitivity of each pad of representative M16 and M4 photomultipliers as determined by illuminating the whole surface.*

from further analysis.

The performance of the RICH detector was also checked by varying the interaction rate of the wire target. In a set of measurements the response of the detector was recorded at target rates from 1 MHz up to the design value of 40 MHz. In Fig. 20, the accumulated number of hits on the photon detector as a function of target interaction rate is presented, and a good linearity can be seen.

Due to non availability of the information from the particle tracking system, the Čerenkov ring radii

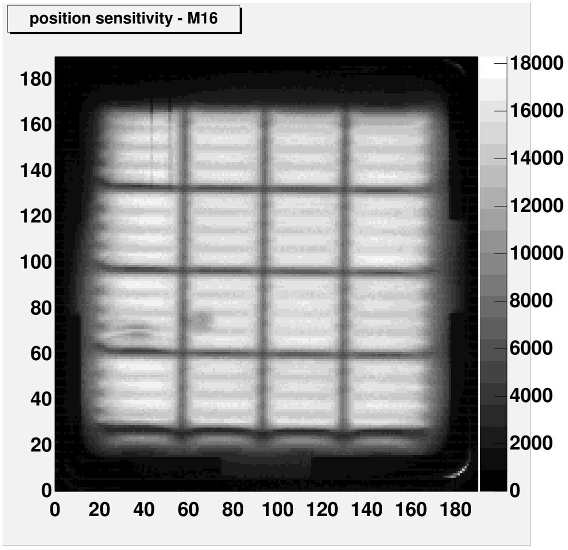


Fig. 17 *Sensitivity of a M16 PMT surface when scanned by a light beam spot of about 20 μm diameter.*

were deduced by finding the rings which best fit the detected hits on the photon detector. Only events which depict well separated Čerenkov rings were employed in a simple analysis [26]. In the analysis one counts the detected photons per Čerenkov ring by looking at appropriate events (two of which are shown in Figs. 21 and 22) and measures the corresponding ring radius. The number of counted hits per Čerenkov ring is plotted as a function of Čerenkov angle in Fig. 23. The lines drawn on the plot correspond to a hypothesis that $31 \pm \sqrt{31}$ photons are radiated from particles approaching the velocity of light.

For each of the rings recorded in Fig. 23, we calculated the photon detector response parameter $N_0$. The resulting distribution is shown in Fig. 24. We observe that the average value of the photon detector response parameter as well as the average number of detected photons per ring are consistent with the expectations.

## V. Summary

A detector of Čerenkov photons for a high rate environment of the HERA-B experiment was designed,

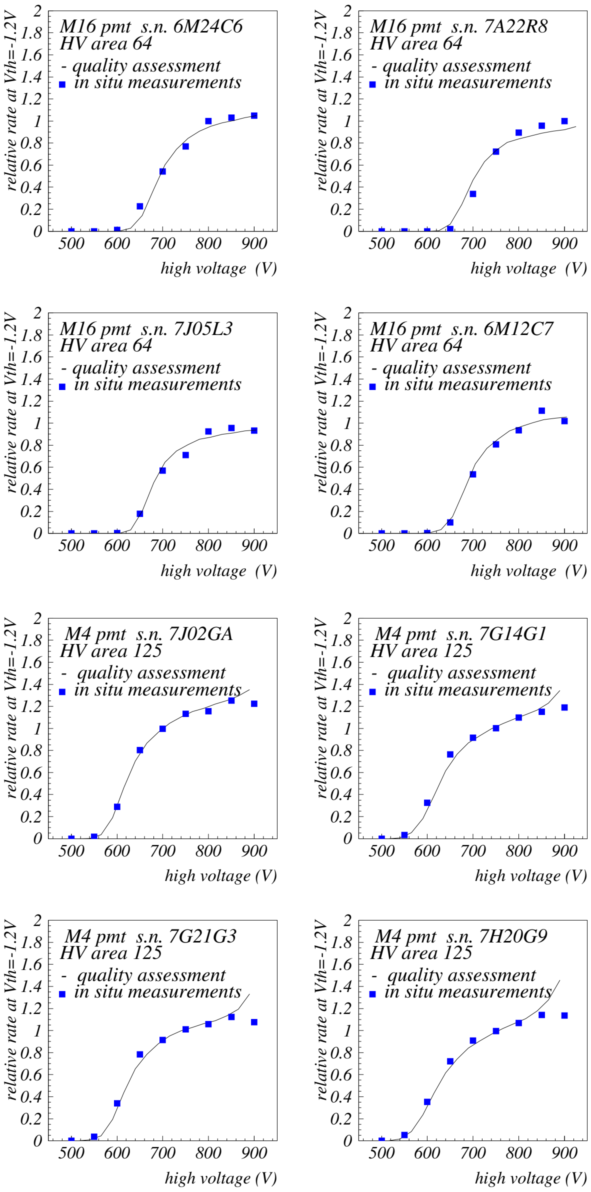


Fig. 18 *The plateau curves for a group of four M16 (top) and a group of four M4 photomultiplier tubes (bottom). The data labelled 'in situ' represent values measured during the photon detector testing in its final position, while the curves labelled 'quality assessment' correspond to measurements made in the laboratory during on-the-bench quality tests. The data are normalised to the average of the three points at 750 V, 800 V and 850 V.*

tested, installed and commissioned. A preliminary data analysis shows that the design goals, a figure of merit $N_0$=43 cm$^{-1}$, resulting in 31 detected photons on a saturated Čerenkov ring, was met. We also note that the resolution as determined from a stand-alone ring search analysis reported elsewhere [27], is consistent

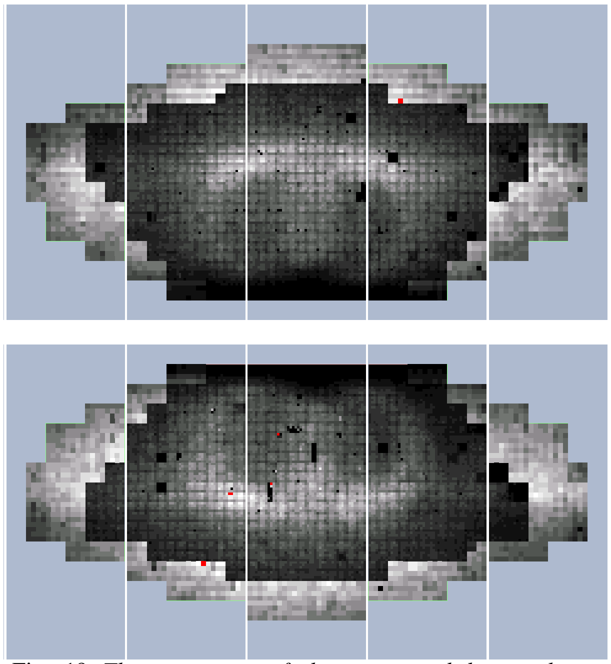

Fig. 19 *The occupancy of the upper and lower photon detectors shows the region occupied by M16 (inner region) and M4 PMT's (outer region).*

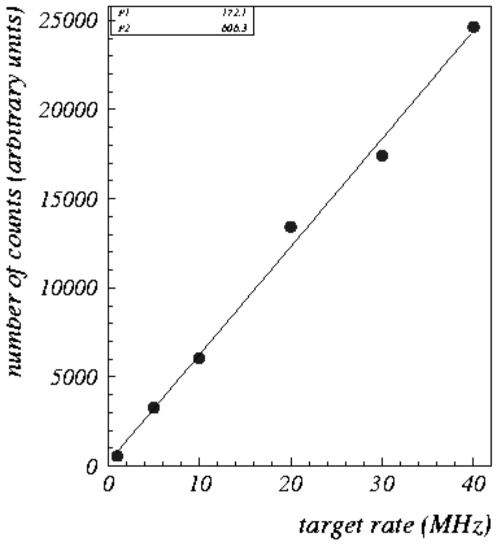


Fig. 20 *Accumulated number of hits on the photon detector versus target interaction rate. Noisy channels (in total about 0.3%) are suppressed.*

with the design value of 0.7 mrad.

## VI. References

[1] T. Lohse et al. Proposal for HERA-B, DESY PRC-94/02, May 1994

[2] P. Križan et al., Nucl. Instr. Meth. in Phys. Res. A351 (1994) 111-131.

[3] J.L. Rosen, Nucl. Instr. Meth. in Phys. Res. A408(1998)191

[4] S. Korpar et al., Nucl. Instr. and Meth. in Phys. Res. **A433** (1999) 128-135

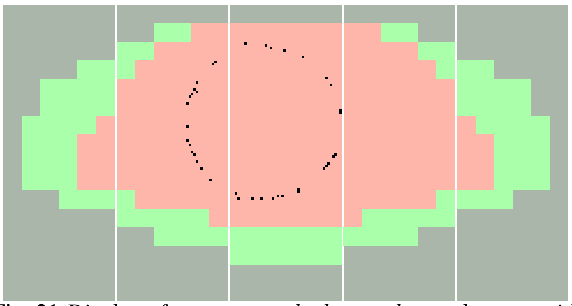

Fig. 21 *Display of an event on the lower photon detector with a single Čerenkov ring consisting of 33 detected photons. From the ring radius Čerenkov angle of* $51.9\ \pm 0.5\,\mathrm{mrad}$ *is deduced for which* $31 \pm 2$ *detected photons would be expected.*

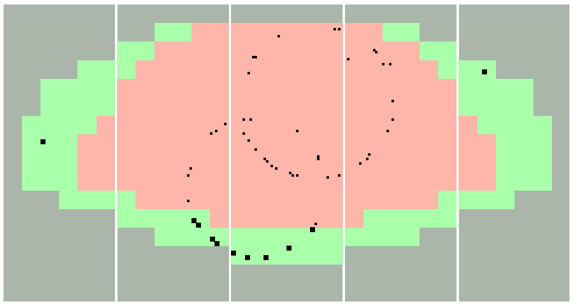

Fig. 22 *Two intersecting Čerenkov rings, one with 22 photons detected by four and sixteen channel photomultiplier tubes, a measured Čerenkov angle of* $45.5\ \pm 0.5\,\mathrm{mrad}$ *and expected number of* $23.8 \pm 1.5$ *hits, and a ring with 27 photons detected exclusively by sixteen channel photomultiplier tubes,* $49.8\ \pm 0.5\,\mathrm{mrad}$ *Čerenkov angle and expected* $28.5 \pm 1.8$ *hits.*

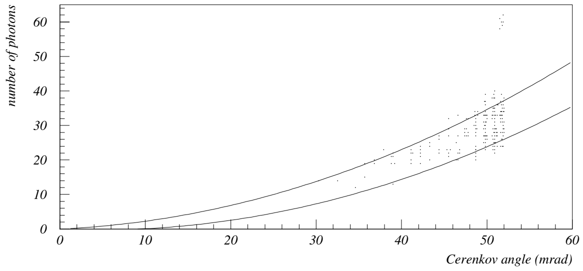


Fig. 23 *Number of detected photons versus Čerenkov angle for nearly 200 rings which could be well separated. Some events are also seen with two times more detected photons per ring than expected. They are due to Čerenkov radiation of an overlapping* $\mathrm{e}^{+}\mathrm{e}^{-}$ *pair.*


[5] J. McGill et al., UT Austin Note

[6] D. Dujmić, K. Reeves, HERA-B RICH Note 97-182, Hamburg 1997

[7] T. Hamacher et al., Nucl. Instr. and Meth. in Phys. Res. **A371** (1996) 289-294

[8] P. Križan, M. Cindro, V. Cindro, S. Korpar, G. Omahen, A. Stanovnik, M. Starič, Nucl. Instr. and Meth. in Phys. Res. **A364** (1995) 243-252

[9] P. Križan, S. Korpar, M. Starič, A. Stanovnik, M. Cindro,


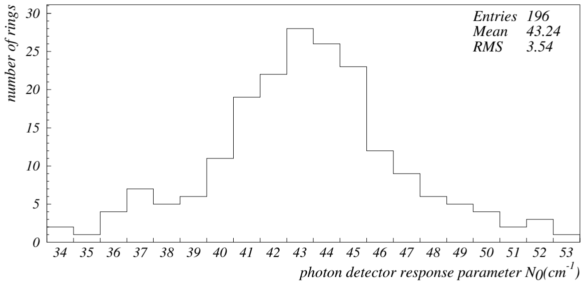


Fig. 24 *The distribution of the photon detector response parameter* $N_0$.


D. Škrk, M. Zavrtanik, T. Hamacher and E. Michel, 1994 IEEE NSS Conference Record, Volume 2 (1995) 985-988

[10] J. Pyrlik at al., Nucl. Instr. and Meth. in Phys. Res. **A414** (1998) 170-181

[11] S. Korpar, P. Križan, A. Stanovnik, M. Starič, D. Škrk, IEEE Transactions on Nuclear Science, Vol. 46, Number 3 (1999) 317-320

[12] P. Križan, S. Korpar, M. Starič, A. Stanovnik, M. Cindro, D. Škrk, M. Zavrtanik, T. Hamacher, E. Michel, Nucl. Instr. and Meth. in Phys. Res. **371** (1996) 151-154

[13] P. Križan et al., Nucl. Instr. and Meth. in Phys. Res. **A387** (1997) 146-149

[14] Hamamatsu Data Sheets for R5900-M16 and R5900-M4 Photomultipliers

[15] J. McGill, R. Schwitters, HERA-B Note 96-278, DESY, Hamburg (1996); D. Broemmelsiek, Nucl. Instr. and Meth. in Phys. Res. **A433** (1999) 136-142.

[16] R. Eckmann, M. Ispirian, S. Karabekyan, J. McGill, R. Schwitters, HERA-B Note 97-162, DESY, Hamburg (1997)

[17] F.M. Newcomer et al., IEEE Transactions on Nuclear Science, **40**,4 (August 1993)630

[18] P. Križan, M. Starič, Nucl. Instr. and Meth. in Phys. Res. **A379** (1996) 124-129

[19] R. Schwitters, HERA-B Note 97-088, DESY, Hamburg (1997); D. Dujmić, R. Schwitters, HERA-B Note 98-052, DESY, Hamburg (1998)

[20] J. Pyrlik and K. Lau, HERA-B Note 97-182, DESY, Hamburg (1997)

[21] P. Križan, S. Korpar, R. Pestotnik, M. Starič, A. Stanovnik, E. Michel, C. Oehser, W. Schmidt-Parzefall, A. Schwarz, T. Hamacher, D. Broemmelsiek, J. Pyrlik, Nucl. Instr. and Meth. in Phys. Res. **A394** (1997) 27-34

[22] V. Cindro, S. Korpar, P. Križan, A. Stanovnik, M. Starič, D. Škrk, Nucl. Instr. and Meth. in Phys. Res. **A337** (1994) 609-612

[23] S. Korpar, R. Pestotnik, P. Križan, IJS Report, IJS-DP-7615, Ljubljana (1997); HERA-B Note 97-079, DESY, Hamburg (1997)

[24] S. Korpar et al., Proc. of the 2nd Conference on Photodetection, Beaune, France, June 1999, to be published in Nucl. Instr. and Meth. in Phys. Res.

[25] S. Korpar et al., IJS Report, IJS-DP, Ljubljana (1999)

[26] D. Škrk, Doctoral thesis, Univerza v Ljubljani, Fakulteta za matematiko in fiziko, Oddelek za fiziko, Ljubljana, June 1999.

[27] R. Schwitters, HERA-B Note 99-215, DESY, Hamburg (1999).